

RESEARCH

Open Access



Evidence for a month-scale ionospheric precursor to large earthquakes as an outcome of dark matter research

Konstantin Zioutas¹, Ekin Akman², Athanasios Argiriou¹, Giovanni Cantatore³, Serkant Ali Cetin⁴, Jinyun Guo⁵, Marin Karuza⁶, Abaz Kryemadhi⁷, Ionel Lazanu⁸, Marios Maroudas^{9*}, Kaan Ozbozduman¹⁰, Mihaela Parvu⁸ and Yannis Semertzidis^{11,12}

*Correspondence:
Marios Maroudas
marios.maroudas@cern.ch

Full list of author information is
available at the end of the article

Abstract

Catastrophic earthquakes (EQs) ($M \geq 8$) and global ionospheric plasma variations exhibit unexpected planetary orbital periodicities that cannot be explained by known (geo)physical processes. In this study, we identify a robust pre seismic signature in the Total Electron Content (TEC) of the ionosphere that precedes major EQs by up to two months. This finding leads to a novel forecasting method for large magnitude events, providing a significant advance warning window. We propose that the underlying causal triggering mechanism for such correlated phenomena fits-in the scenario of gravitational focusing of galactic dark matter (DM) streams by the solar system bodies. In this framework, Earth based observational tools like the global GPS network can serve a dual role: monitoring terrestrial dynamics and acting as possible sensitive detectors for DM. We demonstrate how continuous GPS recordings can be exploited to project, in real time, the likely timing and location of major seismic events. This interdisciplinary approach provides a novel route to enhance the reliability of catastrophic EQ forecasting. Concurrently, it offers a new method for the direct detection of the dark sector following otherwise unexpected planetary dependencies. While the Axion Quark Nugget (AQN) framework provides an interesting basis for these results, the identified precursors remain model-independent.

Keywords Earthquake precursor, Ionosphere, TEC disturbances, Gravitational focusing, Dark matter streams

1 Introduction

Dark matter (DM), first proposed by Zwicky in the 1930s [1], has eluded all attempts at direct detection for over ~ 30 years. Interestingly, beyond solar observables, growing evidence suggests that certain geophysical and atmospheric phenomena, including earthquakes (EQs) and atmospheric anomalies, display unexpected planetary dependencies [2–4]. Such correlations point to an underlying causal mechanism that originates beyond the solar system.



© The Author(s) 2026. **Open Access** This article is licensed under a Creative Commons Attribution 4.0 International License, which permits use, sharing, adaptation, distribution and reproduction in any medium or format, as long as you give appropriate credit to the original author(s) and the source, provide a link to the Creative Commons licence, and indicate if changes were made. The images or other third party material in this article are included in the article's Creative Commons licence, unless indicated otherwise in a credit line to the material. If material is not included in the article's Creative Commons licence and your intended use is not permitted by statutory regulation or exceeds the permitted use, you will need to obtain permission directly from the copyright holder. To view a copy of this licence, visit <http://creativecommons.org/licenses/by/4.0/>.

Interestingly, a recent theoretical model [5, 6] proposes that specific DM candidates known as axion anti-quark nuggets (AQNs), which interact strongly with ordinary matter [6–9], could trigger seismic phenomena. Noticeably, within this framework, the Sun's multifaceted activity also exhibits distinct planetary periodicities, most notably the 11-year solar cycle [10], that remains unexplained since the ~ 1850's within standard (solar) physics. Furthermore, high-precision measurements of Earth's magnetic field [11] offer an additional avenue for detecting DM candidates such as axions, dark photons, and AQNs [6, 8, 9]. These interdisciplinary approaches not only expand the possibilities for direct detection of streaming DM but eventually also for developing practical, society-relevant applications.

Earth-based observational tools such as the global GPS network may serve a dual purpose [12]. Beyond monitoring ionospheric and solid-Earth dynamics, the continuous GPS measurements [13, 14] may act as sensitive detectors of streaming DM by recording the atmospheric response to energy deposition. Of note, a large number of streaming DM axions or WIMPs have been proposed earlier in a cosmological context [15]. The resulting planetary dependencies allow us to determine the origin of potential precursors. Because celestial alignments cannot be explained by internal terrestrial processes, models based solely on inner Earth mechanisms are effectively excluded.

As strongly interacting DM candidates like AQNs transit the atmosphere, they induce ionization that modifies the (local) plasma state. Because the GPS system continuously monitors Total Electron Content (TEC) to calibrate signal delays, it effectively maps these dark sector interactions across a planetary scale. This synergy between fundamental physics and geophysical monitoring can provide a novel and promising route to enhancing the reliability of catastrophic EQ forecasting, advancing both temporal predictions and the ability to constrain the epicentral region.

Historically, EQ occurrences have exhibited non-random distributions [16], including observed correlations with solar [17] and cosmic ray [18] activity. Furthermore, numerous studies have identified short term localized TEC anomalies within the ionosphere occurring hours or days before major ruptures [19, 20]. While these short-term excursions in global electron density are traditionally interpreted through internal lithosphere ionosphere coupling mechanisms, they also support a downward propagating motion that is consistent with the hypotheses of this work [21].

Here, we focus on large EQs providing a potential terrestrial manifestation of dark-sector impact. Such highly energetic events appear to follow overlooked planetary dependencies [2], and remarkably they correlate with variations of the global atmospheric plasma. This apparent coupling between the atmosphere and the Earth's interior hints at a new mechanism that could trigger strong EQs. Building on observation, here we propose potential precursors to catastrophic (magnitude 8+) EQs, offering a long advance warning. We present the first results which show an advance warning of up to two months and demonstrate how continuous global monitoring of GPS and seismic data could ultimately enable real time projections of the likely timing and location of major EQs, validated and trained on existing datasets.

2 Observations

DM has been firmly established through cosmic-scale observations [1]. As argued in Ref [22], it may also manifest within the solar system and influence processes occurring deep within the dynamic Earth and its atmosphere [4, 5]. In this study, we focus on geophysical events like large EQs ($M > 5.2$) occasionally exceeding magnitude 8. These phenomena exhibit new signatures that display unexpected planetary dependencies not accounted for by known physics [22]. The terrestrial signatures of potential interest for this work include:

- Annual temperature excursions in the upper stratosphere, occurring in early January, which show a clear planetary dependency [2, 4].
- Variations in the local and global ionospheric plasma [7, 22, 23] at altitudes above ~ 100 km.
- EQs of magnitude $M \geq 8$, and especially those with $M \geq 8.6$, that show striking spatiotemporal correlations with global ionospheric plasma activity (see Figs. 1, 2 and 3). Additionally, even local plasma structures in two and three dimensions occasionally evolve toward the epicenter (see e.g. [23]), .
- Planetary dependencies in the temporal occurrence of EQs suggesting a potential driver outside the solar system (see Fig. 4).

Planetary relationships are remarkable because no known planetary force exists apart from the extremely feeble gravitational (tidal) effects. The observed relationships therefore call for an alternative explanation that extends beyond conventional geophysical processes. So far, the only viable hypothesis we have involves the gravitational focusing of streaming DM by solar system bodies, including gravitational effects arising from their intrinsic mass distributions [10, 22, 24–28]. Notably, similar behavior is observed in several other local phenomena, reinforcing the idea that such signatures may share a

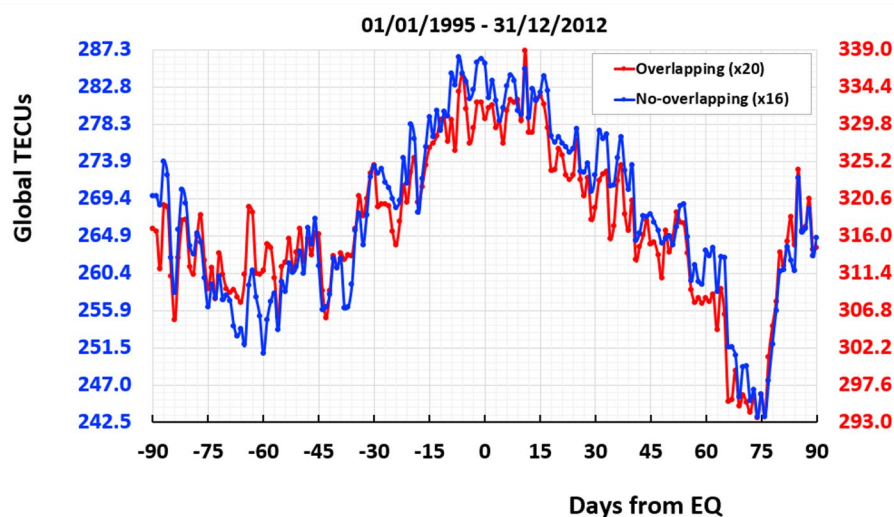


Fig. 1 Global Total Electron Content Units (TECUs) variations before and after catastrophic EQs ($M \geq 8$) between 1995 and 2012. The red curve corresponds to all 20 events, four of which overlapping within ± 90 days, while the blue curve corresponds to the 16 non-overlapping events. Both sets display a slow TEC increase starting about 45 days before a large EQ, indicating a robust pre-seismic signature

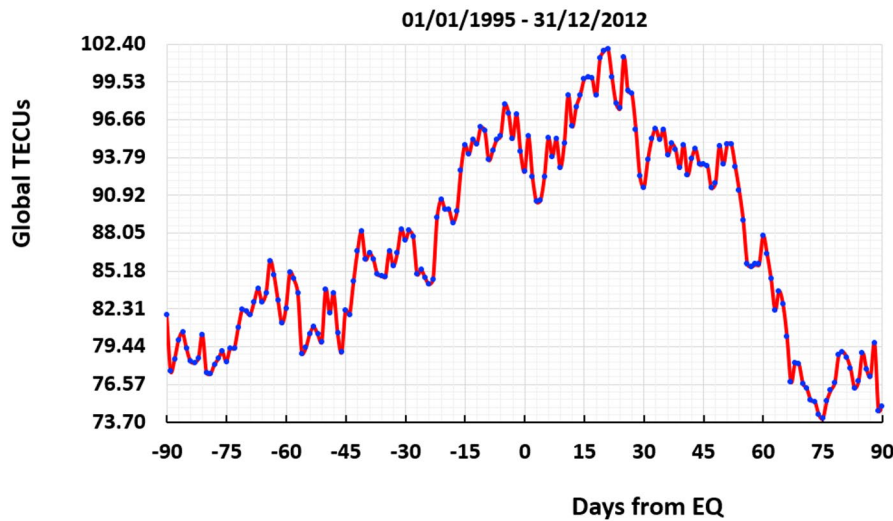


Fig. 2 Global Total Electron Content Units (TECUs) variations before and after the five largest EQs ($M \geq 8.6$) from 1995 to 2012. A pronounced TEC rise appears approximately 1.5 months before an event, confirming a reproducible pre-seismic precursor signal, with a statistical significance of 7.1σ relative to the quiet background measured 60 to 90 days from the events.

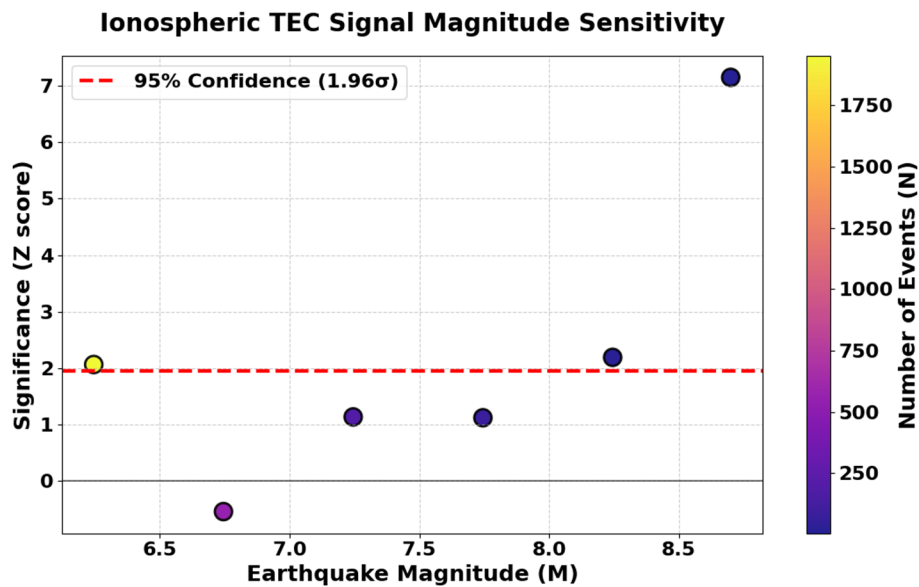


Fig. 3 Scaling of the pre seismic ionospheric signal with EQ magnitude. The statistical significance (Z-score) of the cumulative TEC anomaly is plotted against EQ magnitude (M). The color bar represents the number of events (N) included in each magnitude bin. A pronounced scaling is observed: catastrophic events ($M \geq 8.5$) exhibit a high significance of 7.1σ , while major events ($M = 8.0$ to 8.4) reach 2.19σ . Smaller events ($M < 7.5$) generally remain within the range of stochastic noise ($< 1.96\sigma$), with the significance of the $M \sim 6.2$ bin (2.07σ) being a statistical artifact of the very large sample size ($N = 1,953$) which minimizes background variance. The red dashed line denotes the 95% confidence threshold (1.96σ)

common dark-sector origin. This mechanism may point at a common link among several apparently unrelated terrestrial and atmospheric observables. For an extended discussion, see Ref [22].

A scenario fitting-in the observed correlations between the assumed DM streams [15] and seismicity is provided, unbiased to our work, by the AQN model. Unlike weakly

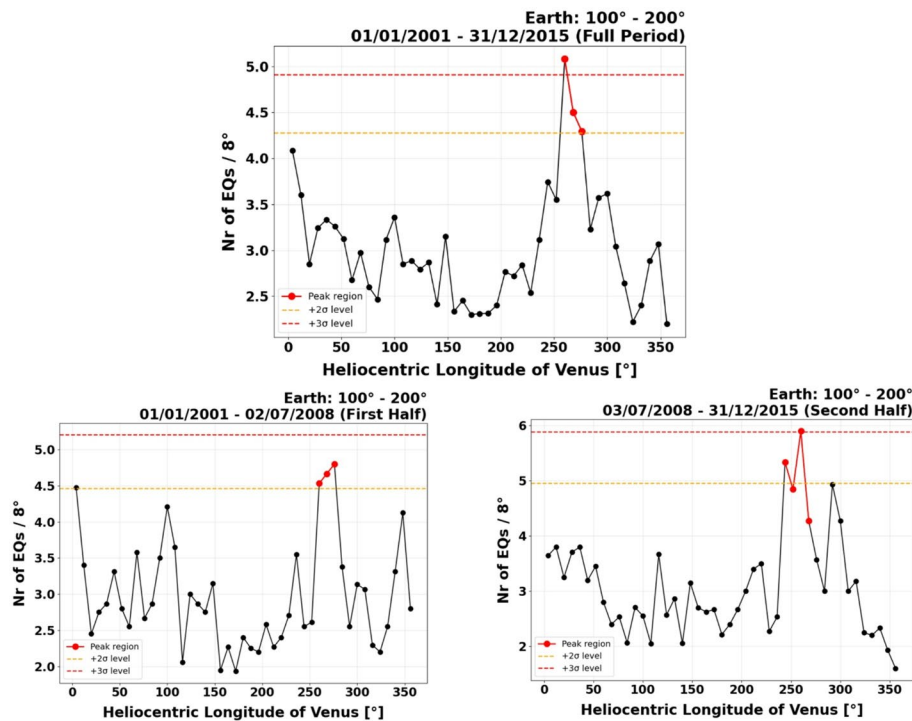


Fig. 4 15,703 stay-days-normalized EQ occurrences with $M > 5.2$ projected onto Venus’s heliocentric longitude, with Earth constrained to 100° – 200° (1 January 2001–31 December 2015). Days with more than 25 EQs were removed to suppress aftershock-driven biases. **Top:** Full dataset, showing an excess near $\approx 260^{\circ}$ with a combined significance of 4.4σ . **Bottom left/right:** First and second half of the dataset exhibit compatible excesses in the same longitude range at the $\sim 4\sigma$ level. The persistence of the signal across each half time intervals excludes systematics with a statistical significance at the 4.4σ level (see e.g. [3]),

interacting DM candidates like axions and hidden photons, AQNs are strongly interacting composites that expect to deposit an enormous amount of energy along their trajectory through the Earth and its atmosphere. While the average DM density is relatively low, gravitational focusing by solar system bodies can enhance the flux of the focused incident stream by several orders of magnitude. As described in [6], the energy deposition rate in the atmosphere is proportional to an enhancement factor $A(t)$, which accounts for the gravitational focusing of streaming DM by solar system bodies. Quantitatively, an expected flux of $0.4/\text{km}^2/\text{year}$ across the Earth total surface area results in approximately 200 million impacts annually, averaging over 500,000 events per day. Because AQNs possess nuclear density and transit the planet at supersonic speeds, the Earth is effectively transparent to their passage, allowing for energy deposition at all depths. Crucially, as an AQN transits the Earth crust at supersonic speeds, it generates significant acoustic overpressure along its Mach cone, being estimated between 0.03 Pa and 0.3 Pa [5]. While this acoustic overpressure is extremely small compared to standard static tectonic stress drops ($O(\text{MPa})$) [29], it falls near the lower threshold of documented dynamic stress perturbations, such as those induced by distant teleseismic surface waves [30] or solid Earth tides [31], that are known to influence seismicity. Furthermore, during periods of planetary alignment, the gravitational focusing of DM streams can amplify the local AQN flux (e.g., the AQNs) by several orders of magnitude. This enhancement subjects the Earth to a concentrated burst of acoustic energy. In lithospheric regions already near a critical metastable state due to long term tectonic

stress, these concentrated overpressure bursts can act as a “small push” or localized trigger that initiates a major seismic event. Within this framework, the observed correlation between ionospheric TEC variations and EQ rates arises naturally: the TEC rise is driven by atmospheric energy deposition, while the EQs could be triggered by the aforementioned acoustic perturbations in the Earth’s crust.

2.1 Ionospheric response

Figures 1 and 2 summarize measured global ionospheric responses associated with the largest EQs. The TEC, where 1 TECU = 10^{16} electrons/m², shows a consistent increase starting about one to two months before a catastrophic event.

To estimate the significance of such trends, we employed Superposed Epoch Analysis (SEA), a standard geophysical method that aligns multiple time-series data to a common reference point (time = 0). This process allows incoherent daily ionospheric fluctuations (noise) to cancel out while amplifying consistent physical signals tied to the seismic events. The original data used in this analysis are derived from the Center for Orbit Determination in Europe (CODE) and contain 6,574 daily averaged measurements of TEC from 01/01/1995 to 30/12/2012.

The 20 largest EQs with magnitude $M \geq 8$ occurring between 1 January 1995 and 31 December 2012 are selected for Fig. 1 (see Table 1). A ± 90 -day window around each EQ is defined, with the EQ date being the reference point (time = 0), to derive the TEC distributions. The red curve represents all 20 events, four of which overlap within the ± 90 -day window. The blue curve shows the 16 non-overlapping events. Both overlapping and non-overlapping EQs exhibit similar long-term behavior, showing a slow increase in global ionospheric electron content starting about 45 days before a large EQ.

To quantify the significance of these peaks, we calculated the Z-score, defined as the difference between the peak value in the analysis window (-45 to +45 days) and the

Table 1 Dates of EQs with $M \geq 8.0$ between 01/01/1995 and 31/12/2012. The table includes the date, magnitude, and geographic location for each catastrophic event

Date	Magnitude	Location
30/07/1995	8,00	Antofagasta, Chile
09/10/1995	8,00	Colima, Mexico
17/02/1996	8,09	Biak region, Indonesia
25/03/1998	8,10	Balleny Islands region
16/11/2000	8,00	New Ireland region, Papua New Guinea
23/06/2001	8,40	near the coast of southern Peru
25/09/2003	8,16	Hokkaido, Japan region
23/12/2004	8,10	north of Macquarie Island
26/12/2004	9,10	2004 Sumatra – Andaman Islands Earthquake
28/03/2005	8,60	northern Sumatra, Indonesia
03/05/2006	8,00	Tonga
15/11/2006	8,30	Kuril Islands
13/01/2007	8,10	east of the Kuril Islands
01/04/2007	8,10	Solomon Islands
15/08/2007	8,00	near the coast of central Peru
12/09/2007	8,40	southern Sumatra, Indonesia
29/09/2009	8,10	Samoa Islands region
27/02/2010	8,80	offshore Bio-Bio, Chile
11/03/2011	9,10	2011 Great Tohoku Earthquake, Japan
11/04/2012	8,60	off the west coast of northern Sumatra

mean of a distal quiet-time baseline (μ_{bg}), normalized by the baseline standard deviation (σ_{bg}). We defined the distal baseline using periods furthest from the seismic event: -90 to -60 days and +60 to +90 days. Using this metric, the 20-event stack yields a significance of 3.7σ .

Fig. 2 applies the same procedure to the five largest EQs with $M \geq 8.6$ during the same period, revealing a similar TEC rise approximately 1.5 months before a large seismic event. Notably, the cumulative anomaly for these five catastrophic events reaches a high significance of 7.1σ relative to the background (-90 to -60 days and +60 to +90 days).

Together, these data indicate a robust, reproducible pre-seismic signature. The fact that the significance scales with EQ magnitude (from 3.7σ at $M \geq 8.0$ to 7.1σ at $M \geq 8.6$) strongly supports a physical coupling between the lithosphere and the upper atmosphere. This is consistent with the hypothesis of this work involving remote exo-solar triggering and downward-propagating effects from an in-falling, low-speed (~ 300 km/s), invisible stream.

To validate these signatures, we evaluated the anomaly using a Monte Carlo simulation by replacing the EQ dates with 1,000 sets of random dates. However, this stochastic shuffling is heavily biased by the 11 year solar cycle, as random selections frequently capture high amplitude solar flares or geomagnetic storms. These solar terrestrial events can increase global TEC by an order of magnitude, creating peaks physically unrelated to seismicity that mask the pre-seismic signal. This solar contamination makes simple Monte Carlo shuffling an inefficient tool for characterizing lithosphere-ionosphere coupling in raw datasets.

We therefore arrive to a more robust physical validation by examining how the ionospheric global plasma scales with EQ magnitude. While random solar storms can produce artificial TEC peaks, solar space weather is completely independent of the energy released by an EQ. Therefore, if the observed TEC rise is associated with seismic activity, the significance of the anomaly should increase proportionally to the energy released in the crust. To test this, we analyzed over 2,800 EQs binned into six magnitude classes from $M = 6.0$ to $M \geq 8.5$.

As shown in Fig. 3, there is indeed a clear pronounced scaling of the Z-score with EQ magnitude. While smaller events ($M < 7.5$) remain largely noise dominated, the significance rises to 2.19σ for major EQs ($M = 8.0$ to 8.4) and reaches a definitive 7.1σ for catastrophic events ($M \geq 8.5$). This magnitude dependent behavior provides strong evidence that the observed TEC rise is a physically coupled response to lithospheric stress accumulation, rather than a stochastic byproduct of solar terrestrial weather.

2.2 Planetary dependency

The high statistical significance of the pre-seismic ionospheric signals (7.1σ) suggests a consistent external driver rather than a purely internal geophysical process. To investigate the origin of this driver, we examine the temporal distribution of EQs in relation to the positions of solar system bodies. This analysis is motivated by the hypothesis that a stream of highly interacting DM particles, like AQNs, enters the solar system from a fixed galactic direction. As planets orbit the Sun, their gravitational fields act occasionally as lenses, focusing an aligned DM stream [15] into high density “caustics” [28] that intersect Earth’s orbit. If some DM over-densities trigger seismic activity through

dark-sector interactions in the Earth's interior, the frequency of EQs should show a measurable dependency on the heliocentric longitude of the lensing planet(s).

Below we test this by projecting the global EQ catalog onto the orbital position of Venus to identify potential spatial clustering. Figure 4 shows the number of EQs projected onto Venus's heliocentric longitude, using a bin size of 8° (≈ 5 days), normalized by the planetary residence time in each bin to eliminate eccentricity effects. To isolate the lensing effect, Earth's position is restricted to a specific orbital sector between 100° – 200° . The emergence of a strong clustering signal within this window effectively points to the specific direction and geometry of the incoming galactic DM stream relative to the solar system.

The selected dataset covers 15 years from 1 January 2001 to 31 December 2015 and originally included 16,396 EQs with $M > 5.2$, spanning 5478 days with an average of 3 EQs per day and magnitudes ranging from 5.2 to 9.0 (average $M \sim 5.6$). Days with more than 25 EQs, attributed mainly to aftershocks, were excluded, removing 10 days ($\approx 0.2\%$) and leaving 15,703 events ($\approx 96\%$ of the original dataset).

The resulting distribution exhibits a pronounced excess near a heliocentric longitude of $\approx 260^\circ$, extending over three adjacent bins (~ 15 days). Using a Z-score formalism based on the mean and standard deviation of the normalized EQs-per-day distribution, the significance of the excess is 4.42σ for the full dataset. To exclude systematics behind the signal, the data were divided into two independent temporal subsets, shown in Fig. 4 bottom. For the first half (1 January 2001–2 July 2008), the same longitude range (260° – 276°) yields a significance of 3.94σ for the three points, while for the second half (3 July 2008–31 December 2015), a slightly shifted but overlapping interval (240° – 268°) gives a significance of 4.29σ for the four points. The persistence of a statistically significant excess across independent time periods demonstrates that the effect is not driven by a small subset of events but reflects a robust feature of the data, excluding thus systematics.

To assess whether the observed clustering could arise from random fluctuations, the distribution of daily EQ counts was compared to a Poisson expectation with the same mean rate (Fig. 5). While the observed distribution is broadly Poisson-like, it exhibits deviations indicative of overdispersion for values above 10 EQs/day. This justifies the use of empirical rate-normalized significance estimates rather than assuming ideal Poisson statistics when evaluating heliocentric longitude clustering. Notably, the global feature of Fig. 4 remains if we exclude days with events more than 10 per day (not shown here). This strengthens the significance of our conclusion, by excluding events which do not follow the Poisson distribution (Fig. 5).

2.3 Periodogram analysis

To distinguish between local gravitational forces and external galactic drivers, we apply a Lomb Scargle periodogram analysis to the global EQ catalog. In standard geophysics, a lunar driven seismicity is expected at the 29.53 day synodic period, which represents the cycle of lunar phases and the resulting gravitational tidal stresses on Earth's crust. Conversely, a signal at the 27.32 day sidereal period, which is the time it takes the Moon to return to the same position relative to the distant stars, would indicate a modulation that depends on Earth's orientation within a fixed external field, such as a galactic DM stream. The absence of a synodic peak and the dominance of a sidereal peak would

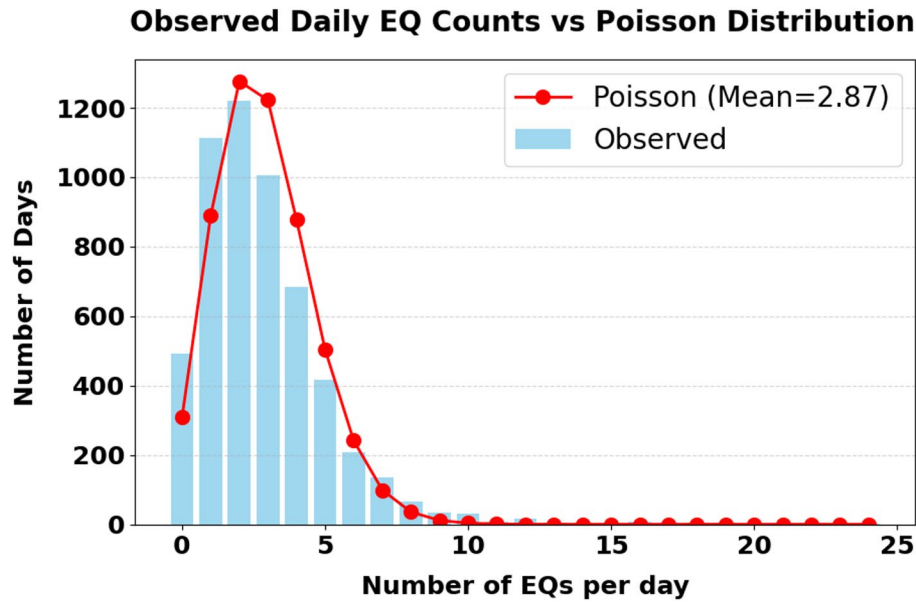


Fig. 5 Distribution of the daily number of EQs with $M > 5.2$ from 1 January 2001 to 31 December 2015, after excluding days with more than 25 events / day. The dataset comprises a total of 15,703 EQs recorded over 5468 days. The empirical mean and variance indicate moderate overdispersion relative to a Poisson process, providing statistical context for the clustering observed in Fig. 4

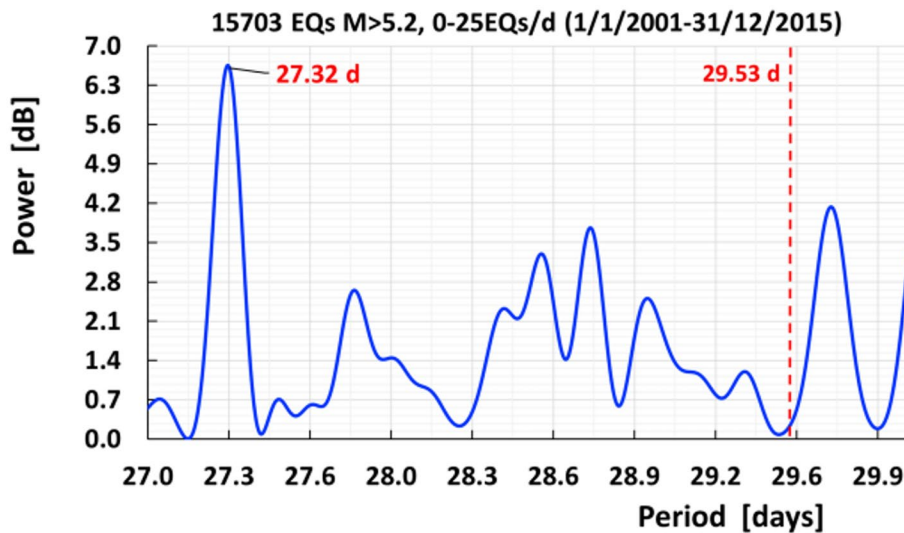


Fig. 6 Lomb-Scargle periodogram of global EQs from 1 January 2001 to 31 December 2015 with magnitude $5.2 < M < 9$, excluding days with over 25 events to suppress aftershocks. The dominant peak at 27.32 ± 0.05 days, exhibiting a statistical significance of 7.4σ , aligns with the sidereal lunar rhythm, while the absence of the 29.53-day synodic peak excludes a possible impact by the lunar gravitational tidal force [22]

therefore provide a “smoking gun” for an exo-solar origin, as tidal forces do not follow sidereal timing.

Figure 6 shows the Lomb-Scargle periodogram of global EQs for the same filtered large EQ dataset as before. The dominant peak at 27.32 ± 0.05 days coincides with the sidereal lunar rhythm, while the absence of the 29.53-day synodic peak excludes the usual lunar tidal forcing as the source of the modulation. To quantify the statistical relevance of the sidereal peak, its power was compared to the local spectral background

in the surrounding period range. As mentioned already before, this approach accounts for the non-Poissonian noise floor inherent in seismic catalogs, providing a more robust baseline than global estimates. More specifically, the peak power (P_{peak}) was compared against the mean (μ_{local}) and standard deviation (σ_{local}) of the spectral power within a local window (24–30 days), excluding the immediate vicinity of the peak. The peak at 27.32 days exceeds the local mean power by 7.4σ ($Z = [P_{\text{peak}} - \mu_{\text{local}}] / \sigma_{\text{local}}$), demonstrating that it represents a highly exceptional feature of the spectrum rather than a stochastic fluctuation of the background noise. The dominance of this sidereal peak, along with the absence of a synodic signal, this result supports the hypothesis that external factors of exo-solar system origin, influence both ionospheric and lithospheric processes.

Combining the results of Figs. 4 and 6, the cumulative statistical significance of these independent planetary and lunar-sidereal periodicities is well above 5σ , providing compelling evidence that the modulation of large EQs is driven by factors of exo-solar system origin.

3 Discussion-conclusion

The results of this work reveal a reproducible temporal relationship between global ionospheric plasma variations and the onset of largest EQs ($M \geq 8$ and $M \geq 8.6$), pointing at an early-warning time of roughly 1.5–2 months (Figs. 1 and 2). This constitutes a first societally relevant outcome of our study: the temporal behavior of the ionospheric plasma tracks the onset of a major EQ with month-scale lead times.

A crucial finding in this analysis is the clear magnitude sensitivity of the ionospheric anomaly. As demonstrated in Fig. 3, the statistical significance of the pre-seismic peak scales with the energy released in the crust, rising from roughly 2σ for moderate events to over 7σ for catastrophic ruptures. This scaling provides a vital physical validation that distinguishes the seismic signal from stochastic ionospheric noise. Furthermore, while solar activity is a primary driver of ionospheric variability, the TEC does not always follow solar indices linearly, as other factors do occasionally mask routine solar variations [32, 33]. This observed decoupling suggests the presence of an independent external driver, which we associate in our scenario with focused incident DM streams.

Comparing our global observations with established regional case studies provides further insight into the physical scaling of these anomalies. Documented case studies demonstrate that regional TEC measurements are highly sensitive to local tectonic settings and remain crucial for the spatial localization of events hours or days prior to a rupture [19, 20, 34]. Similarly, recent investigations of moderate EQs in North Africa, including the $M = 5.7$ Ain Temouchent event [35] and the $M = 6.4$ Al Hoceima event [36], report regional TEC precursor lead times ranging from a few days to roughly two weeks. The temporal variance between the roughly 45 days for catastrophic $M \geq 8$ events and 14 days for moderate $M \sim 6$ events could reflect a physical scaling governed by EQ magnitude. Within standard tectonic models [37], the spatial extent of the preparation zone and the duration of the critical pre-rupture phase scale directly with the energy release. Therefore, a massive EQ event might require a much longer preparation period of structural destabilization compared to a moderate regional event. As a result, the atmospheric disturbances generated during this buildup phase could appear significantly earlier for larger magnitude ruptures.

Furthermore, methodological factors and background ionospheric variability likely play a role in this temporal discrepancy. As shown in Fig. 3, the statistical significance of the global TEC anomaly is highly sensitive to the EQ magnitude. For moderate EQs, the precursor development might begin much earlier than two weeks. However, the initial perturbations are likely too weak to overcome background ionospheric noise, only becoming detectable above the background noise in the final days when local tectonic stress reaches the critical failure threshold. Additionally, this difference in timing highlights the fundamental contrast between observing local networks and averaging data globally. Our global TEC methodology captures the earlier, broader atmospheric perturbations and enhances planetary-scale exo-solar signals while averaging out localized variations. In contrast, regional GNSS networks are optimized to detect localized lithospheric coupling driven by specific tectonic settings, making them highly sensitive to the final micro-fracturing processes occurring near the epicenter.

In addition to these temporal signatures, the analysis uncovers unexpected planetary dependencies. Namely, EQ occurrence clusters within specific heliocentric longitudes, e.g. of Venus (Fig. 4). The analysis remained consistent when the dataset is split into two halves (01/01/2001–02/07/2008 and 03/07/2008–31/12/2015), with the peaks around 260° showing each a significance of about 4σ , reinforcing the planetary dependency as a reproducible feature rather than a random statistical fluctuation. This planetary clustering also provides an important methodological validation. Although the long-term averaging of the SEA mitigates randomly distributed geomagnetic storms, residual non-linear space-weather artifacts could persist. However, standard geomagnetic disturbances, such as those tracked by Kp and Dst indices, are driven by solar dynamics and are entirely independent of planetary positions. Consequently, they cannot explain the spatial clustering relative to Venus, which lacks an intrinsic magnetic field, confirming the pre-seismic signal cannot be of solar origin. Nevertheless, to further isolate future early-warning simulations from extreme geomagnetic events, subsequent analyses may explicitly integrate Kp and Dst masking.

Additionally, EQs with $M > 5.2$ follow a clear lunar sidereal periodicity (27.32 days), while the synodic month (29.53 days) is absent (Fig. 6). The missing synodic signal, despite the well-known dominance of synodic tidal forcing, shows that the observed dependencies cannot be explained by conventional geophysical mechanisms or known planetary forces in our vicinity. Furthermore, the highly resolved 27.32 days peak cannot be attributed solely to the solar synodic rotation [38]. Since the Sun exhibits differential rotation between approximately 25 and 32 days, a global solar space weather driver would produce a correspondingly broad terrestrial signal (spanning several days rather than ~ 0.1 days). Generating such a sharp peak would require an unknown mechanism to consistently isolate roughly 1.4% of the solar surface over a 15-year period, excluding a purely solar origin. On the other hand, terrestrial models like the Lithosphere Atmosphere Ionosphere Coupling (LAIC) propose Radon release as a primary ionospheric precursor [39]. However, as an intrinsic geological process, Radon emission does not fit in the 27.32 days sidereal periodicity or the planetary clustering observed in this study. The absence of a 29.53 days synodic peak further suggests that these correlations are not driven by lunar tidal forces, requiring an extrinsic driver, with the streaming DM underlying this proposal being a possible mechanism. Together, these atmospheric and lithospheric signatures form a coherent pattern pointing to a remote external driver

modulating both ionospheric plasma and seismicity (for more cases see ref [22]). Such a scenario suggests that streaming DM may independently influence both the upper atmosphere [4, 7] and inner Earth seismicity, consistent with the observed planetary dependencies (Figs. 4 and 6). Consequently, the ionospheric and lithospheric signatures could be parallel manifestations of the same external driver. This possibility would account for the observed precursors without necessarily requiring a direct physical coupling between the upper atmosphere and the Earth interior.

The presence of robust and repeated pre-seismic signature suggests a clear practical potential. By combining the continuous global plasma monitoring with archival EQ records, it becomes feasible to construct simulations with real data capable of estimating, in real time, the likely timing, approximate epicentral region and eventually the magnitude of a future large EQ. Such simulations could incorporate the spatiotemporal evolution of ionospheric plasma distributions, which in several historical cases developed toward the eventual epicenter. Prior studies already indicate a correspondence between plasma structures and EQ locations [23], encouraging more elaborated future simulations. As further datasets accumulate, forecast precision will improve, offering thus a novel, data-driven method for EQ prediction that leverages existing observational infrastructure in a parasitic yet effective manner. Within this framework, local GNSS networks and global ionospheric maps serve complementary roles. While local data are crucial for analyzing co-seismic disturbances, global TEC monitoring provides a broader perspective for identifying month-scale precursors. Notably, this applied perspective emerges as a byproduct of a study originally motivated by a fundamental physics question, namely the detection of DM in observations from outer space.

The full set of observations, including the temporal relationships, the planetary dependencies, and the atmospheric–lithospheric coherence, is difficult to reconcile within known physics. At present, the most viable mechanism capable of naturally accounting for these diverse signatures is streaming DM which is gravitationally focused by solar-system bodies towards the Earth. Such a mechanism has been previously invoked to explain similar periodicities in other solar-system observables. In particular, the AQN model by A. Zhitnitsky provides a scenario in which strongly interacting DM composites may occasionally trigger seismicity [5, 6]. It is worth stressing here that these would serve as initiators rather than energy sources; the energy released in an EQ remains governed by long-term geological stress accumulation. Nevertheless, AQNs offer a rare framework capable of integrating the full range of observations, many of which remain unexplained within standard geophysics. While the AQN framework is a leading candidate that also addresses broader cosmological mysteries, such as the matter-antimatter asymmetry, these seismic findings may be compatible with other dark sector constituents such as magnetic monopoles or dark photons. Consequently, the identified precursors remain fundamentally independent of the specific DM model.

In conclusion, parasitic monitoring of Earth's dynamic upper atmosphere and its interior effectively transforms our planet with its atmosphere into a precursor for major EQs. Our analysis is carried out model-independently, strengthening its robustness. The AQN framework seems to provide a natural way to explain the diverse observational signatures mentioned in this work, suggesting a possible connection between fundamental physics and emergent Earth-system behavior.

Acknowledgements

We thank the referees for their comments which helped a lot to revise the manuscript. K.Z. wishes to thank the CAST collaboration at CERN, the actual roots of this work, and also CERN people for inspiring discussions including the continuous help by the CERN librarians. We acknowledge financial support from the Open Access Publication Fund of Universität Hamburg. M.M. acknowledges funding from by the Deutsche Forschungsgemeinschaft (DFG, German Research Foundation) under Germany's Excellence Strategy – EXC 2121 “Quantum Universe” – 390833306, and through the DFG funds for major instrumentation grant DFG INST 152/824-1.

Author contributions

Conceptualization: K.Z. Investigation: K.Z., M.M. Methodology: K.Z., M.M. Data curation: M.M. Formal Analysis: M.M., K.Z. Visualization: M.M., I.L., K.Z. Validation: K.Z., E.A., A.A., G.C., S.A.C., J.G., M.K., A.K., I.L., M.M., K.O., M.P., Y.S. Writing and editing the manuscript: K.Z., E.A., A.A., G.C., S.A.C., J.G., M.K., A.K., I.L., M.M., K.O., M.P., Y.S.

Funding

Open Access funding enabled and organized by Projekt DEAL. This research did not receive any specific grant from funding agencies in the public, commercial, or not-for-profit sectors.

Data availability

The list of EQs used in this work has been acquired from the “U.S. Geological Survey (USGS) Earthquake Hazards Program”, part of the “National Earthquake Hazards Reduction Program (NEHRP)” led by the “National Institute of Standards and Technology (NIST)”. The data have been downloaded from the publicly available “Advanced National Seismic System (ANSS) Comprehensive Earthquake Catalog”: <https://earthquake.usgs.gov/earthquakes/search/>. The data for the global electron content of the ionosphere are derived from the “Center for Orbit Determination in Europe (CODE)”: <http://ftp.aiub.unibe.ch/> & <https://doi.org/10.1002/2014JA019977>. Finally, the data with Venus heliocentric longitude positions have been downloaded from Caltech/Jet Propulsion Laboratory (JPL)'s Horizons System of National Aeronautics and Space Administration (NASA) <https://ssd.jpl.nasa.gov/horizons.cgi>.

Declarations

Ethics approval and consent to participate

Not applicable.

Consent for publication

Not applicable.

Competing interests

The authors declare no competing interests.

Author details

¹Physics Department, University of Patras, Patras-Rio 26504, Greece

²Department of Physics, University of California, Berkeley, USA

³Physics Department, University & INFN of Trieste, Trieste 34127, Italy

⁴Department of Basic Sciences, Istinye University, Istanbul 34396, Türkiye

⁵College of Geodesy/Geomatics, Shandong University Science and Technology, Qingdao 266590, China

⁶Faculty of Physics, University of Rijeka, Rijeka 51000, Croatia

⁷Physics Department, Messiah University, Mechanicsburg, PA 17055, USA

⁸Faculty of Physics, University of Bucharest, MG-11, Magurele-Bucharest, Romania

⁹Institute for Experimental Physics, University of Hamburg, 22761 Hamburg, Germany

¹⁰Physics Department, Bogazici University, 34342 Istanbul, Türkiye

¹¹Department of Physics, KAIST, Daejeon 34141, Korea

¹²Present address: Physics Department, Brookhaven National Laboratory, Upton, NY 11973, USA

Received: 25 December 2025 / Accepted: 11 May 2026

Published online: 15 May 2026

References

1. Zwicky F. Die Rotverschiebung von extragalaktischen Nebeln. *Helv Phys Acta*. 1933;6:110. <https://doi.org/10.48550/arXiv.1711.01693>.
2. Maroudas M. Signals for invisible matter from solar-terrestrial observations, Ph.D. thesis, University of Patras, 2022; <https://arxiv.org/abs/2404.02290>
3. Zioutas K, Anastassopoulos V, Argiriou A, Cantatore G, Cetin SA, Gardikiotis A, Hoffmann DHH, Hofmann S, Karuza M, Kryemadhi A, Maroudas M, Matteson EL, Ozbozduvan K, Papaevangelou T, Perryman M, Semertzidis YK, Tsagris I, Tsagris M, Tsiledakis G, Utz D, Valachovic E. The dark universe is not invisible. *Phys Sci For*. 2021;2(1):10. <https://doi.org/10.3390/ECU2021-09313>.
4. Zioutas K, Argiriou A, Fischer H, Hofmann S, Maroudas M, Pappa A, et al. Stratospheric temperature anomalies as imprints from the dark universe. *Phys Dark Universe*. 2020;28:100497. <https://doi.org/10.1016/j.dark.2020.100497>.
5. Budker D, Flambaum VV, Zhitnitsky A. Infrasonic, acoustic and seismic waves produced by the axion quark nuggets. *Symmetry*. 2022;14. <https://doi.org/10.3390/sym14030459>.
6. Zhitnitsky A, Maroudas M. Mysterious anomalies in Earth's atmosphere and strongly interacting dark matter. *Symmetry*. 2025;17:79. <https://doi.org/10.3390/sym17010079>. <https://arxiv.org/abs/2405.04635v3>.

7. Bertolucci S, Zioutas K, Hofmann S, Maroudas M. The sun and its planets as detectors for invisible matter. *Phys Dark Universe*. 2017;17:13. <https://doi.org/10.1016/j.dark.2017.06.001>.
8. Zhitnitsky A. Nonbaryonic dark matter as baryonic colour superconductor. *JCAP*. 2003;0310:010. <https://doi.org/10.1088/1475-7516/2003/10/010>. <https://arxiv.org/abs/hep-ph/0202161v4>.
9. Zhitnitsky A. Solar flares and the axion quark nugget dark matter model. *Phys Dark Universe*. 2018;22:1. <https://doi.org/10.48550/arXiv.1801.01509>. <https://arxiv.org/abs/1801.01509>.
10. Zioutas K, Tsagri M, Semertzidis YK, Papaevangelou T, Hoffmann DHH, Anastassopoulos V. The 11 years solar cycle as the manifestation of the dark universe. *Mod Phys Lett A*. 2014;29:1440008. <https://doi.org/10.1142/S0217732314400082>.
11. Friel M, Gjerloev JW, Kalia S, Zamora A. Search for ultralight dark matter in the SuperMAG high-fidelity dataset. *Phys Rev*. 2024;D110:115036. <https://doi.org/10.1103/PhysRevD.110.115036>.
12. Zioutas K et al. Atmospheric Temperature anomalies as manifestation of the dark Universe. Proceedings 15th Intern. Conf. on Meteorology, Climatology and Atm. Phys. COMEAP, (2021), Ioannina, Greece; <https://www.conferre.tv/comecap2020> p.728.
13. Jin S, Occhipinti G, Jin R. GNSS ionospheric seismology: Recent observation evidences and characteristics. *Earth Sci Rev*. 2015;147:54–64. https://www.ipgp.fr/~ninto/Jin_2015ESR.pdf.
14. Jin S, Wang Q, Dardanelli G. A Review on Multi-GNSS for Earth Observation and Emerging Applications. *Remote Sens*. 2022;14(16):3930. <https://doi.org/10.3390/rs14163930>.
15. Vogelsberger M. S.D.M. <>White 2011 Streams and caustics: the fine-grained structure of Λ CDM haloes. *MNRAS* 413 1419 <https://doi.org/10.1111/j.1365-2966.2011.18224.x> <https://arxiv.org/abs/1002.3162v2>.
16. Bendick R, Bilham R. Do weak global stresses synchronize earthquakes? *Geophys Res Lett*. 2017;44(16):8320–7. <https://doi.org/10.1002/2017GL074934>.
17. Marchitelli V, Harabaglia P, Troise C, De Natale G. On the correlation between solar activity and large earthquakes worldwide. *Scientific Reports*, 10, 1, p. 11495, (2020); <https://www.nature.com/articles/s41598-020-67860-3>.
18. Homola P, et al. Observation of large scale precursor correlations between cosmic rays and earthquakes with a periodicity similar to the solar cycle. *J Atmos Solar Terr Phys*. 2023;247:106068. <https://doi.org/10.1016/j.jastp.2023.106068>.
19. Oikonomou C, Haralambous H, Pulinetis S, Khadka A, Paudel SR, Barta V, Muslim B, Kourtidis K, Karagioras A, Inyurt S. Investigation of Pre-Earthquake Ionospheric and Atmospheric Disturbances for Three Large Earthquakes in Mexico. *Geosciences*. 2021;11(1):16. <https://doi.org/10.3390/geosciences11010016>.
20. Oikonomou C, Haralambous H, Muslim B. Investigation of ionospheric TEC precursors related to the M7.8 Nepal and M8.3 Chile earthquakes in 2015 based on spectral and statistical analysis. *Nat Hazards*. 2016;83(Suppl 1):97–116. <https://doi.org/10.1007/s11069-016-2409-7>.
21. Zioutas K et al. Fingerprints of the dark Universe from geoscience, Proceedings of the 1st Mediterranean Geosciences Union International Conference, Springer, (2024); https://doi.org/10.1007/978-3-031-43218-7_96
22. Argiriou A et al. Novel Dark Matter Signatures, PoS COSMICWSPers2024 (2025) 035/1.474.0035; <https://doi.org/10.48550/arXiv.2501.15498>.
23. Zhou Y, Yang J, Zhu F, Su F, Hu L, Zhai W. Ionospheric disturbances associated with the 2015 M7.8 Nepal earthquake, *Geodesy. Geodynamics*. 2017;8:221. <https://doi.org/10.1016/j.geog.2017.04.004>.
24. Kryemadhi A, Maroudas M, Mastronikolis A, Zioutas K. Gravitational focusing effects on streaming DM as a new detection concept. *Phys Rev*. 2023;D108:123043. <https://doi.org/10.1103/PhysRevD.108.123043>.
25. Hoffmann DHH, Jacoby J, Zioutas K. Gravitational lensing by the sun of non-relativistic penetrating particles. *Astropart Phys*. 2003;20:73. [https://doi.org/10.1016/S0927-6505\(03\)00138-5](https://doi.org/10.1016/S0927-6505(03)00138-5).
26. Patla BR, Nemiroff RJ, Hoffmann DHH, Zioutas K. Flux enhancement of slow-moving particles by Sun or Jupiter: Can they be detected on Earth? *ApJ*. 2013;780:158. <https://doi.org/10.1088/0004-637X/780/2/158>.
27. Sofue Y. Gravitational focusing of low-velocity dark matter on the Earth's surface. *Galaxies*. 2020;8(2):42. <https://doi.org/10.48550/arXiv.2005.082>.
28. Prézeau G. Dense dark matter hairs spreading out from Earth, Jupiter, and other compact bodies. *ApJ*. 2015;814:122. <https://doi.org/10.1088/0004-637X/814/2/122>.
29. Allmann BP, Shearer PM. Global variations of stress drop for moderate to large earthquakes. *J Geophys Res*. 2009;114:B01310. <https://doi.org/10.1029/2008JB005821>.
30. Gombert J, Johnson P. Seismology: dynamic triggering of earthquakes. *Nature*. 2005;437:830. <https://doi.org/10.1038/437830a>.
31. Ide S, Yabe S, Tanaka Y. Earthquake potential revealed by tidal influence on earthquake size–frequency statistics. *Nat Geosci*. 2016;9:834–7. <https://doi.org/10.1038/ngeo2796>.
32. Rich FJ, Sultan PJ, Burke WJ. The 27-day variations of plasma densities and temperatures in the topside ionosphere. *J Geophys Research: Space Phys*. 2003. <https://doi.org/10.1029/2002JA009731>.
33. Yasyukevich Y, et al. Ionospheric Global and Regional Electron Contents in Solar Cycles 23–25. *Symmetry*. 2023;15(10):1940. <https://doi.org/10.3390/sym15101940>.
34. Ikuta R, Hisada T, Karakama G, Kuwano O. Stochastic evaluation of pre-earthquake TEC enhancements. *J Geophys Research: Space Phys*. 2020. <https://doi.org/10.1029/2020JA027899>, 125, e2020JA027899.
35. Tachema A, Nadji A, Bezzeghoud M. Geodetic analysis for investigating possible seismo-ionospheric precursors related to the Ain Témouchent earthquake of December 22, 1999, in NW Algeria. *Arab J Geosci*. 2022;15(1270). <https://doi.org/10.1007/s12517-022-10533-4>.
36. Tachema A, Nadji A, Sondhiya DK. Space-based GNSS radio signals to investigate ionospheric plasma changes preceding the 2016 Al Hoceima-Morocco earthquake, Mw = 6.4. *Ann Geophys*. 2023;66(6):SE643. <https://doi.org/10.4401/ag-8901>.
37. Dobrovolsky IP, Zubkov SI, Miachkin VI. Estimation of the size of earthquake preparation zones. *Pure appl Geophys*. 1979;117(5):1025–44. <https://doi.org/10.1007/BF00876083>.
38. Anagnostopoulos G. The sun as a significant agent provoking earthquakes. *Eur Phys J Spec Top*. 2021;230:287–333. <https://doi.org/10.1140/epjst/e2020-000266-2>.

39. Pulinetis S, Ouzounov D. Lithosphere–atmosphere–ionosphere coupling (laic) model – an unified concept for earthquake precursors validation. *J Asian Earth Sci.* 2011;41:371–82. <https://doi.org/10.1016/j.jseaes.2010.03.005>.

Publisher's Note

Springer Nature remains neutral with regard to jurisdictional claims in published maps and institutional affiliations.